A numerical study on the effects of charge air temperature on the combustion and emission characteristics of a marine generator engine

Pham Van Chien, Ngo Duy Nam*

Ho Chi Minh City University of Transport
*Email: nam.ngo@ut.edu.vn (Corresponding author)

Abstract: A numerical study was carried out to investigate the effectiveness of the charge air cooling method on the exhaust gas emission reduction when applied to a four-stroke marine generator diesel engine at full load. The AVL FIRE 2018a software was used to perform three-dimension (3D) simulations of the combustion process and emission formations inside the engine cylinder operating with various charge air temperatures (CATs). The simulation results were then verified by measured values obtained from experiments in the Green Ship Technology laboratory (GSTLab), Korea. The simulation results showed In-Cylinder peak pressure increase tendencies as the CAT decreased from 360 K to 320 K, leading to an increase in the brake mean effective pressure (BMEP) by 10.74%. At the same time, the In-Cylinder peak temperature was decreased, resulting in a reduction in NO emission by 33.85%. Soot, CO, and CO_2 emissions were also reduced by 63.92, 44.66, and 3.22%, respectively. In addition, the CAT cooling method also reduced specific fuel oil consumption (SFOC) by 9.68% due to the increase in the indicated efficiency. This study would be a useful material for operating engines in cases of trying to reduce exhaust gas emissions from existing engines without any additional emission post-treatment device.

Keywords: Charge air cooling; combustion; emission; nitric oxide; CO; CO_2; soot; CFD analysis.

1. Introduction

Due to the increasing environmental hazards of marine engine exhaust emissions as well as the International Maritime Organization (IMO) emission regulations are becoming increasingly strict, reducing exhaust gas emissions from marine engines is mandatory for new and existing vessels in use [1]. Figure 1 shows stricter regulations on NOx emission from ships, in which 80% NOx emission from ships must be cut off from January of 2016 [2].

Theoretically, marine exhaust gas emission reduction approaches are divided into three categories, including (1) pre-treatment; (2) internal treatment; and (3) post-treatment [3]. Figure 2 shows a summary of exhaust gas emission reduction approaches applied on MAN B&W engines [3].

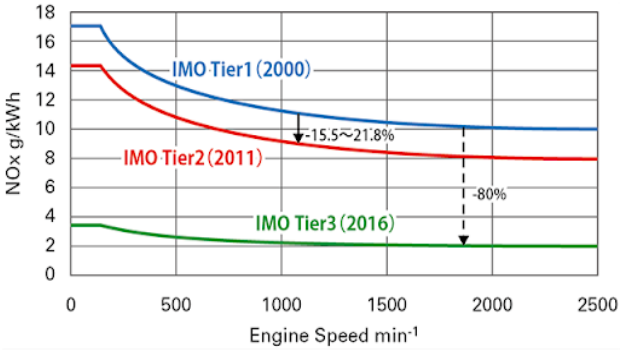

Figure 1. IMO's regulation on NOx emission [2].

In pre-treatment approaches, fuels, the main factor that affect the engine's combustion and emission characteristics are substituted or handled prior to being supplied to engines. Regarding substitute fuels, various gas fuels are currently being increasingly employed in marine engines to reduce engine exhaust gas emissions. LNG (composed of mainly methane - CH_4), ethane (C_2H_6), LPG (composed of mainly

propane - C_3H_8), butane (C_4H_{10}), dimethyl ether (DME)… have been proven to be suitable diesel alternatives in diesel engines to reduce exhaust emissions while maintaining engine power [1] [4]-[17]. Effects of various gaseous alternative fuels on emission characteristics of marine engines can be found in our previous study [18]. Another way to pre-treat fuels is emulsifying liquid fuels by water to create emulsified fuels. Water in emulsified fuels will get the heat of combustion gas inside the engine cylinder to evaporate, resulting in a reduction in the In-Cylinder peak temperature and thus NO emissions. This approach had demonstrated advantages in terms of exhaust gas emission reductions, however, engines need to be modified to use alternative gaseous fuels which have low cetane number (low reactivity fuels). Modifying diesel engines into dual-fuel (DF) engines for instance.

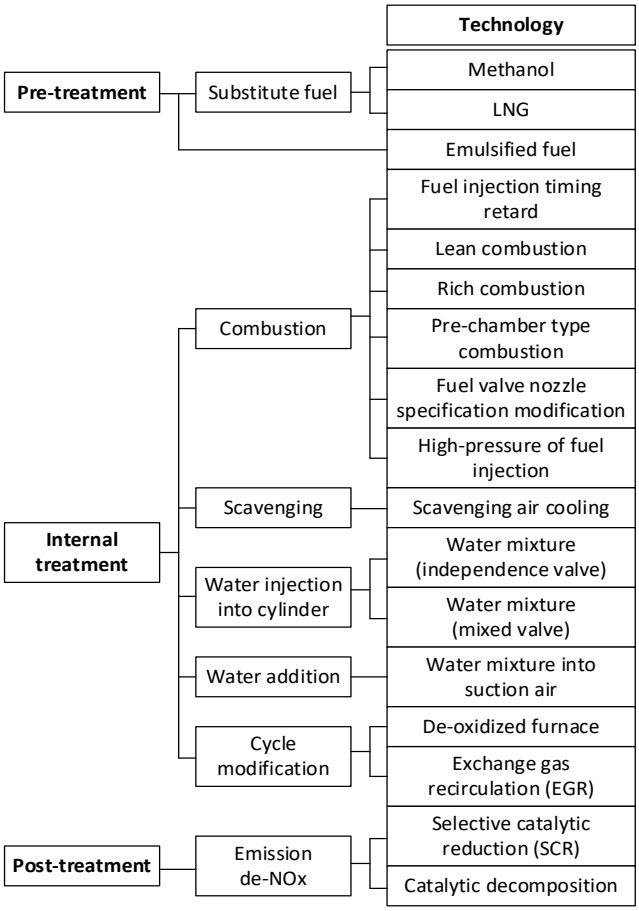

Figure 2. Exhaust gas emission reduction technologies from marine diesel engines [2].

In internal treatment approaches, the combustion of fuel inside the engine cylinder will be modified towards the goal of achieving lower exhaust gas emissions. Using fuel injection timing adjustment, injection strategy modification, lean or rich combustions, pre-chamber type combustion, etc. are examples of this method. The effectiveness of the multiple injection strategies on exhaust gas emission reduction in marine engines can be found in our previous study [19]. In addition, the method of adding water to the engine combustion chamber to reduce the peak temperature in the cylinder or modifying the engine working cycle (exhaust gas recirculation - EGR is an example) is also an effective way to reduce emissions. They are also being effectively used in the marine industry today. In post-treatment approaches, it is necessary to equip exhaust gas post-treatment devices to treat the exhaust gas after it has left the engine. Using a selective catalytic reduction (SCR) system for NOx reduction is an example of this method. These methods don't require modifications on fuels or existing engines, but

exhaust gas post-treatment devices are mandatory. This increases additional costs and makes the engine room become more cramped.

Among the mentioned exhaust gas reduction approaches, charge air cooling, one of the internal treatment methods, has been found as the simplest method to reduce effectively engine exhaust gas emissions without any modification on fuels, engines as well as using any post-treatment device. In addition, it can be easily applied to any existing engine by simply adjusting the CAT cooling system to reduce CAT [20]-[23].

In order to better understand the effects of CAT on the combustion process and emission characteristics of the engine, we performed numerical simulations of the combustion inside the engine cylinder of a four-stroke generator diesel engine at the full load with various CATs. The AVL FIRE R2018a simulation software with its state-of-the-art models has been proven to be suitable for simulating combustion and emission formation inside gasoline, diesel, and DF engines with high accuracy [24]. Therefore, this software was used to perform 3D simulations to calculate the combustion process and emission formations inside the engine cylinder. The combustion process of the engine with five various CATs was simulated to analyze the effects of CAT on the In-Cylinder pressure, temperature, and emission characteristics. The simulation results were then verified by measured values obtained from experiments in the Green Ship Technology laboratory (GSTLab), Busan, Korea.

2. Numerical analysis

2.1. Engine specifications and simulation conditions

The object of this research was a four-stroke generator diesel marine engine. The engine has V-type 4-stroke 8-cylinders with a cam-driven fuel oil supply system. And it is charged with inter-cooled compressed air supplied by two exhaust-gas turbochargers. The specifications of the engine are shown in table 1.

In this study, numerous simulations of the combustion process of the engine running with various CATs at the full load were simulated. The simulation results among all simulation cases were then compared to analyze the effects of CAT on the In-Cylinder temperature, pressure, and emission characteristics of the engine. The results are presented in detail in section 3.

Table 1. Simulated engine specifications.

Parameters	Value	Unit
Manufacturer	Doosan, Korea.	
Engine type	4-stroke, V-type, 8-cylinder, Turbocharged & Intercooler	
Power x rpm @ 100% load	484 kW @ 1800 rpm [33.1 kW/liter @ 1800rpm]	
BMEP	2.3	MPa
SFOC	129.8	Liters/h
Bore x Stroke	128 x 142	mm
Displacement	14.618	liters
Compression ratio	14.6:1	
Injection nozzle	Multi-hole type	
IVC	36^0	ABDC
EVO	62^0	ATDC

2.2. CFD simulation models

The AVL FIRE simulation software with its state-of-the-art models has been proven to be suitable for simulating combustion and emission formation inside gasoline, diesel, and DF engines with high accuracy [24]. The AVL FIRE ESE Diesel platform was used to models the working process of the engine from the intake valve closing (IVC) to the exhaust valve opening (EVO). The simulation process consisted of three

steps: (1) pre-processing, (2) processing, and (3) post-processing. The first step included declaring general engine parameters, building computational domains, creating movable computational meshes, and setting up the simulation parameters. The solutions were calculated in the second step. In the third step, the simulation results were analyzed and reported. After obtaining the simulation results, the simulation results and measured results were compared for the validation purpose of the simulation models. This process was repeated until the simulation and measured results matched.

The k-zeta-f turbulence model was used to simulate the turbulence of the fluid flow inside the engine cylinder. This is a four-equation turbulent model, so it had higher precision and better stability than the k–ε two-equation model [25]. In the CFD method, the mixing and transports of chemical species in combustion problems will be modeled by solving equations of conservations describing diffusion, the convection phenomenon, reaction sources, and concentrations for each component species. Therefore, species transport models must be used in conjunction with combustion models to model combustion problems. In this study, the species transport model provided by AVL FIRE in conjunction with the extended coherent flame model (ECFM) [26][27] was used to simulate the combustion process occurring inside the engine cylinder. The species transport model and the ECFM are presented in detail in Appendix A and B, respectively, in our previous research [28]. The diesel nozzle flow sub-model [27][29] was used to simulate the fuel injection process. This model offers a simple method to correct the injection velocities and initial droplet diameters due to cavitation. The breaking up and evaporation phenomena of fuel droplets were simulated using the WAVE and Dukowicz sub-model respectively [27][29]. The Auto-Ignition model [27] was used to simulate the self-ignition phenomenon of the diesel fuel that occurs in a fuel direct injection diesel engine.

To model NO formation inside the engine cylinder the extended Zeldovich mechanism has been used [27][30][31]. This chemical reaction mechanism comprises seven species and three reactions and has been proven to be able to highly accurately predict thermal NO formation inside engine cylinders over a wide range of equivalence ratios. The kinetic soot mechanism [27][30] was used to simulate the soot formation owing to the combustion process. The extended Zeldovich model and kinetic soot mechanism have been presented in detail in Appendix C and D, respectively, in our previous research [28]. The Walljet1 sub-model [27][29] was used to simulate the interaction between the fuel droplets and walls. Other CFD models can be found in the literature [27][29][30]. Table 2 summarises the numerical models used in this study.

Table 2. Summary of the numerical models.

Model	Description	
Turbulence	k-zeta-f	
Combustion	Standard Species Transport Model	
	Extended Coherent Flame Model - ECFM	
Emission	NO	Extended Zeldovich model
	Soot	Kinetic Soot formation model
Ignition	Auto-Ignition Model	
Atomization	Breakup	WAVE model
	Evaporation	Dukowicz Model
	Droplet-wall interaction	Walljet1 model

2.3. Computational mesh, boundary, and initial conditions

The AVL FIRE ESE-Diesel platform was used to build a 2D engine combustion chamber geometry

and then create a computational mesh for the CFD analysis. Owing to the axial symmetry of the engine combustion chamber, the fuel nozzle of the engine had 12 identical holes, and to reduce the calculation time, only $1/12^{th}$ of the entire 3D computational mesh of the combustion chamber was generated. The calculation was performed in series using a twelve-core processor and took approximately 36 h of CPU time. Figure 3 shows $1/12^{th}$ of the entire 3D computational mesh of the combustion chamber at 25 crank angle degrees (CAD) after the top dead center (ATDC).

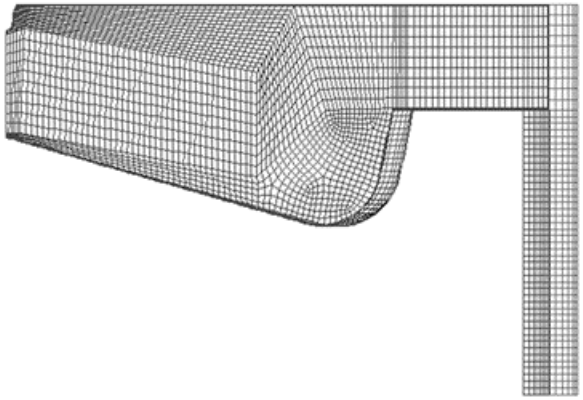

Figure 3. One-twelfth portion of the entire 3D computational mesh of the combustion chamber at 25 CAD ATDC.

The boundary conditions (BCs) of the cylinder head, piston surface, and cylinder liner were defined as impermeable wall BCs. The cylinder geometry was symmetric around the cylinder axis; thus, the cyclic BCs were assigned to the cutting surfaces of the computational domain. The simulation started from the IVC of 35 CAD after the bottom dead center (ABDC) (IVC = 35 CAD ABDC) to the EVO of 62 CAD before the bottom dead center (BBDC) (EVO = 62 CAD BBDC). The starting of injection (SOI) of the diesel fuel was taken at 12 CAD BTDC. The fuel injection duration of the engine was 7.5 ms. This means that the diesel fuel injection occurs in 32 CAD, from 12 CAD BTDC to 20 CAD ATDC. The BCs and initial conditions for the numerical simulation cases were derived from experiments in GSTLab and were shown in table 3.

Table 3. BCs and initial conditions for CFD analysis.

BCs	Boundary Type/Condition
Piston surface	Mesh movement/Temp./570.15 K
Cylinder liner	Wall/Temp./470.15 K
Cylinder head	Wall/Temp./570.15 K
Segment cut	Periodic/Inlet/outlet
Initial Conditions	Value
Charge air temp.	47, 57, 67, 77 and 87 ^{0}C
Charge air press.	3 Bar
IVC	35 CAD ABDC
EVO	62 CAD BBDC
SOI	12 CAD BTDC
Injection duration	7.5 milliseconds (32 CAD)

2.4. CFD simulation model validations

The simulation results were verified by comparing them with the measured results obtained from engine experiments in GSTLab in the case of the CAT of 47^0C.

The comparisons between the simulation and experiment results of the engine are shown in figure 4 below. It is obvious that the simulation and experiment results are in good agreement. In terms of brake mean efficient pressure (BMEP) and indicated specific power, the deviations between the simulated and experiment were only 3.35% and 4.35%, respectively, whereas the deviations between the simulated and experimental brake specific fuel oil consumption (BSFOC) was 3.48%.

These deviations are reasonable and prove the accuracy of the CFD simulation models. After validating the CFD simulation models, the validated models were applied to simulate the combustion and emission formations inside the engine cylinder in all cases of CAT.

3. Simulation results

To clearly illustrate the effects of CAT on combustion and emission formations inside the engine cylinder, all the BCs and working conditions of the engine were remained unchanged, except for the difference in the CAT. In this section, the In-Cylinder pressure, temperature, and emissions in all simulation cases are presented and analyzed.

3.1. In-Cylinder fluid flow turbulence

Basically, the mean turbulence kinetic energy (TKE) reflects the turbulence intensity of the fluid flow inside the engine cylinder. TKE is the average kinetic energy in one unit of mass associated with eddies in turbulent flows in fluid dynamics. Physically, TKE is characterized by the fluctuations of the measured root-mean-square (RMS) velocities.

According to the Reynolds and Navier–Stokes equations, the TKE can be calculated by turbulence models, which are built based on the closure method. In general, the TKE is defined as half the sum of the velocity component variances (square of standard deviations), as shown in equation (1) [32]:

$$k = \frac{1}{2}\left(\overline{(u')^2} + \overline{(v')^2} + \overline{(\omega')^2}\right), [\frac{m^2}{s^2}] \qquad (1)$$

In Equation (1), k, u', v', and ω' denote the TKE and the turbulent part of the horizontal (x- and y-axis) and vertical (z-axis) velocities of turbulence flow respectively. TKE is proportional to the square of the turbulence velocity components. In another word, TKE intensity indicates the intensity of the turbulence of the fluid flow in the engine cylinder. Higher TKEs indicate higher turbulence intensities of fluid flows.

The mean TKEs of the fluid flow in the engine cylinder for all simulation cases are shown in figure 5. The simulation results showed that the maximum TKE decreased as the CAT decreased. This implies that the turbulence velocity of the fluid flow in the engine cylinder would be decreased if we reduce the CAT.

The reasons may be due to the reduction in the reaction rate when the air temperature is reduced. The forward reaction rate for reaction r, k_f, r is computed using the Arrhenius expression (2):

$$k_{f,r} = A_r T^{\beta_r} e^{-E_a/RT} \qquad (2)$$

Where A_r is Arrhenius pre-exponential factor; β_r is temperature exponent; E_a is activation energy; R is the universal gas constant; T is the absolute temperature. According to equation (2), it is obvious that the reaction rate will be decreased if the temperature decreases. This results in a reduction in the maximum TKE as shown in figure 5.

3.2. In-Cylinder pressure

The simulated In-Cylinder pressure diagrams for all the simulation cases are shown in Figure 6. The simulation results showed that the In-Cylinder pressure peak was increased as CAT decreased. This is because the ignition delay (ID) time was longer when the CAT was decreased (figure 8).

As has been known, the diesel droplets need time to receive heat for heating and vaporization, the diesel will not ignite immediately but after a few moments, which is the ID time. During the ID time, the injected diesel droplets will mix with air in the cylinder, forming a pre-mixed (diesel–air) mixture. The ID time will become longer if the CAT is lower.

The longer the ID time, the more fuel accumulates in the engine cylinder. Additionally, a longer ID time will shift the starting of combustion (SOC) closer to the top dead center (TDC). More accumulated fuel ignites closer to the TDC resulting in an increase in the In-Cylinder pressure peaks as shown in figure 6. This phenomenon was also reported in [30][31].

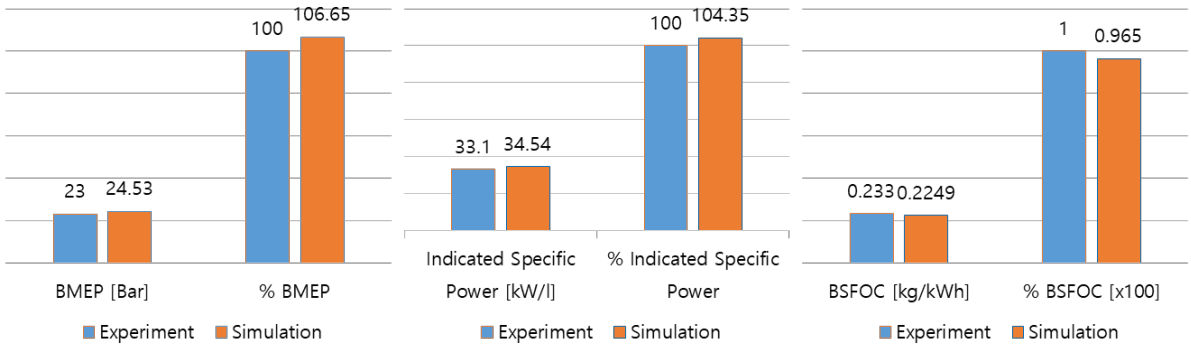

Figure 4. Comparisons of simulation and experimental results.

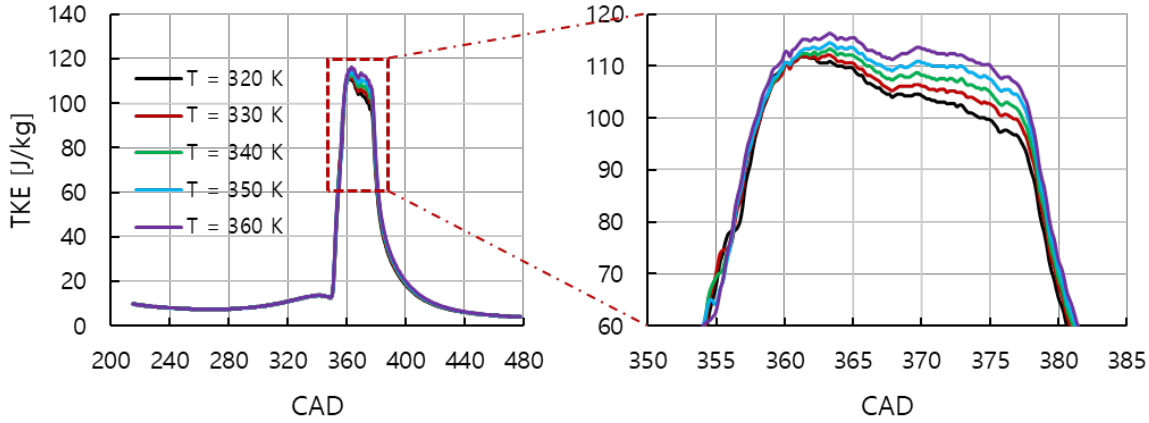

Figure 5. Mean TKEs of the fluid flow inside the engine cylinder in all simulation cases.

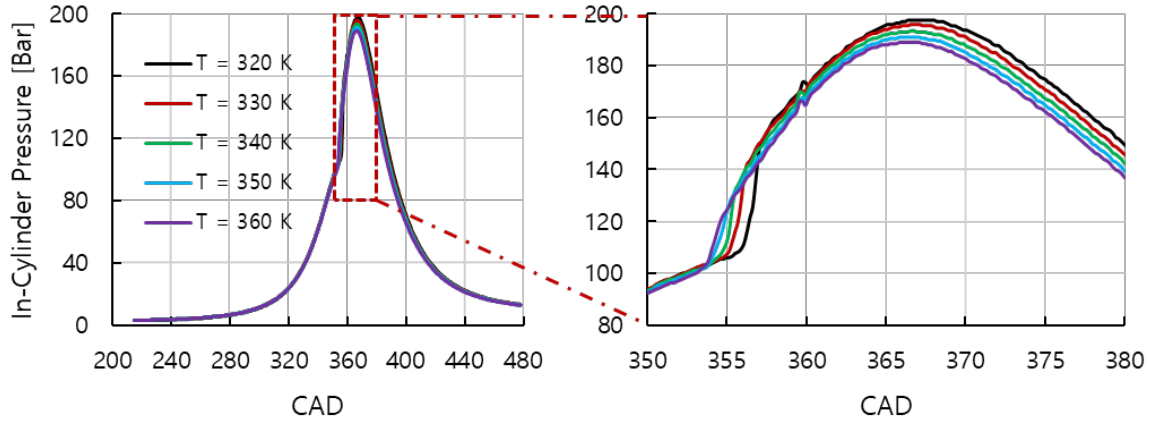

Figure 6. Mean In-Cylinder pressure diagrams in all simulation cases.

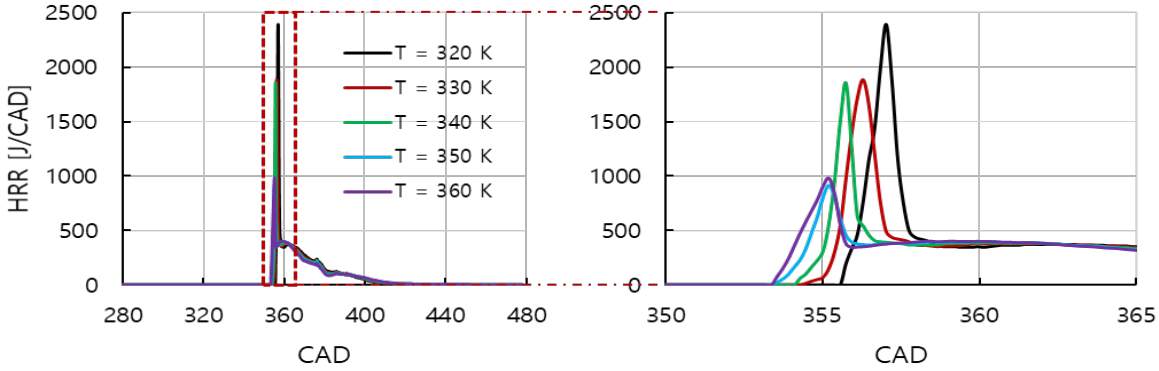

Figure 7. HRR diagrams in all simulation cases.

Analyzing the heat release rate (HRR) of combustions reinforces the above statement. As can be seen in figure 7, it is obvious that the HRR increased as the CAT decreased. In addition, the ID time was longer when the CAT was reduced. As HHR strongly depends on the burnt fuel amount, more heat will be released if there is more fuel accumulated in the engine cylinder for combustions. A longer ID time due to a lower CAT causes more fuel to accumulate in the engine cylinder during the ID period. As a result, more fuel ignites resulting in an increase in the HRR. Finally, more heat releases closer to the TDC resulting in an increase in the In-Cylinder pressure peak as mentioned above.

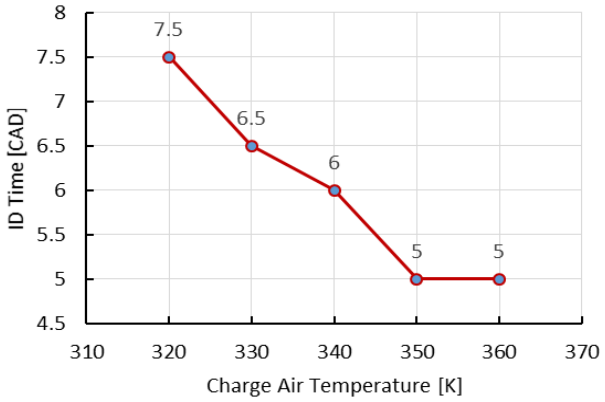

Figure 8. ID time according to CAT.

3.3. In-Cylinder Temperature and NO Emission

The In-Cylinder temperature diagrams of all simulation cases are shown in figure 9. The simulation results showed reduction tendencies in the In-Cylinder peak temperature when the CAT was decreased. The same tendency was also reported in [20][23][33][34]. Physically, the compression temperature at the end of the compression process is proportional to the charge air temperature (the temperature of the air at the start of compression). Therefore, the compression temperature was decreased as the CAT decreased. As a result, the peak temperature was reduced accordingly as shown in figure 9.

Figure 10 shows the NO emissions generated in all the combustion gases. It is obvious that the NO emission was decreased as the CAT decreased. It is universally known that NO is the main component and usually occupies more than 90% of NOx emissions generated from internal combustion engines. Two typical chemical mechanisms are involved in NO formation: the thermal mechanism (Zeldovich mechanism) and the prompt mechanism (Fenimore mechanism). Indirect fuel injection diesel engines, only the NO thermal mechanism must be considered. Therefore, the extended Zelodovich NO emission model was used to simulate the NO formation in this study. According to the thermal mechanism, NO formation is considerably influenced by the In-Cylinder peak temperature and oxygen (O_2) concentration within the engine cylinder. NO formation occurs in regions in the cylinder where the local temperature is above 1800 K, and the formation rate increases significantly with an increase in the In-Cylinder peak temperature [27][35]. As shown in figure 9, the In-Cylinder peak temperature was decreased as the CAT decreased from 360 K to 320 K, resulting in a decrease in the NO emission by 33.85% as shown in figure 10. This is the main purpose of reducing the CAT.

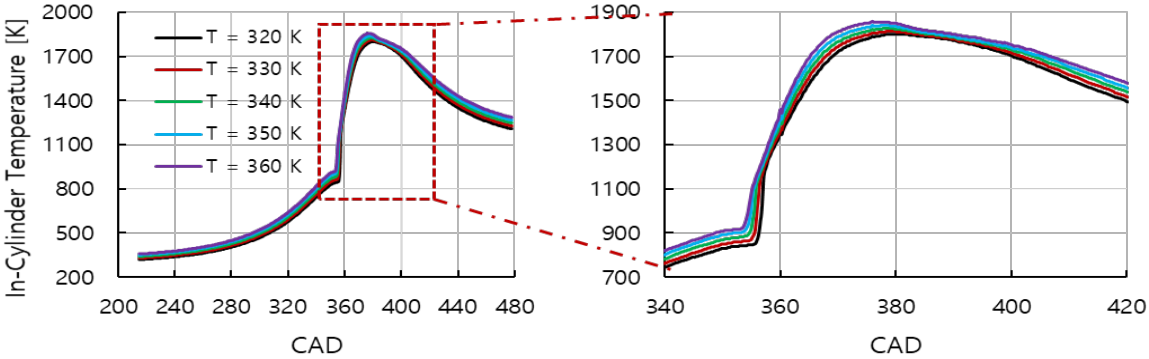

Figure 9. Mean In-Cylinder temperature according to CAT.

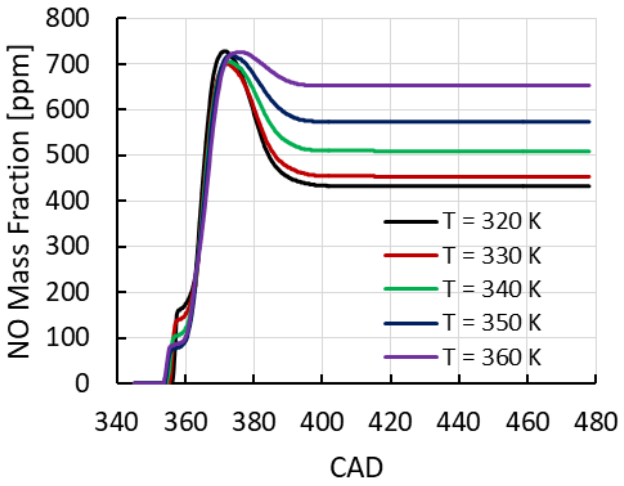

Figure 10. Mean NO mass fractions according to CAT.

3.4. Soot Formation

Soot is the main component of PM emissions [36]–[39]. Under high temperature and equivalence ratios (fuel-rich conditions), which are typically found in diesel diffusion combustions, hydrocarbon fuels have a strong tendency to form carbonaceous particles, that is soot. Under normal running conditions of engines, most soot formed in the early combustion stages is burnt due to oxidation with O_2 in oxygen-rich areas inside the combustion chamber in the later stage of combustions. In diesel engines, the completeness of the soot oxidation process and thus the final generated amount of soot actually determine their particle emission characteristics [30]. The local equivalence (fuel/air) ratio (C/O and C/H-ratio), pressure, temperature, and residence time play the most important role during the soot formation of engines [30]. Soot particles are formed very early in the diffusion combustion process because of the dissociation of fuels under high temperature and high equivalence ratio conditions.

Chemically, under ideal conditions, the oxidation of hydrocarbon fuels and O_2 forms CO_2 and H_2O. The amount of oxygen necessary for complete oxidations is called the stoichiometric O_2 requirement $O_{2,\,stoichiometric}$, and can be calculated based on the following reaction equation [30]:

$$C_nH_mO_k + \left(n + \frac{m}{4} - \frac{k}{2}\right) O_2 \rightarrow nCO_2 + \frac{m}{2}H_2O \quad (3)$$

Where k, n, and m respectively are the number of oxygen (O), carbon (C), and hydrogen (H) atoms of the reacting fuel.

The actual amount of O_2 available for combustion is expressed by the excess air ratio λ or by its inversion, the equivalence ratio ϕ:

$$\phi = \frac{1}{\lambda} = \frac{O_{2,stoichiometric}}{O_2} \quad (4)$$

Figure 11 shows the mean soot mass fraction in the engine cylinder according to the engine CADs in all combustion cases. The simulation results showed a reduction tendency in soot formation when the CAT decreased. The same tendency was also reported in [35][36]. As widely known, soot is mostly formed in the fuel-rich regions of combustions and strongly depends on local equivalence ratio (or excess air ratio) and temperature. As CAT decreased, the air density increased accordingly, resulting in an increase in the fresh air amount supplied to the engine cylinder. A higher supplied air amount resulted in an increase in the excess air ratio, as shown in figure 12. A higher excess air ratio (or a lower equivalence ratio) in the 320 K case resulted in a reduction in the soot emission by 63.92% compared with the case 360 K as shown in figure 11.

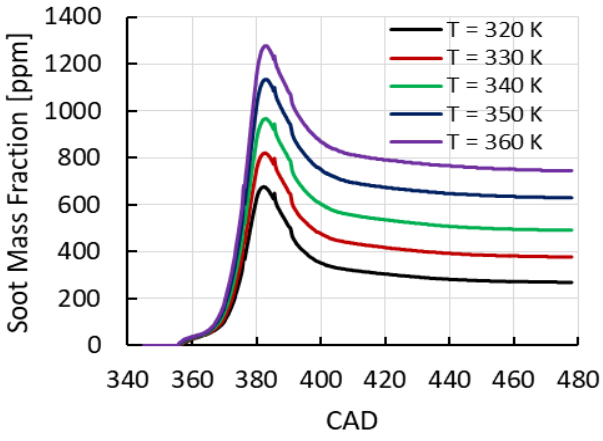

Figure 11. Mean soot mass fractions according to CAT.

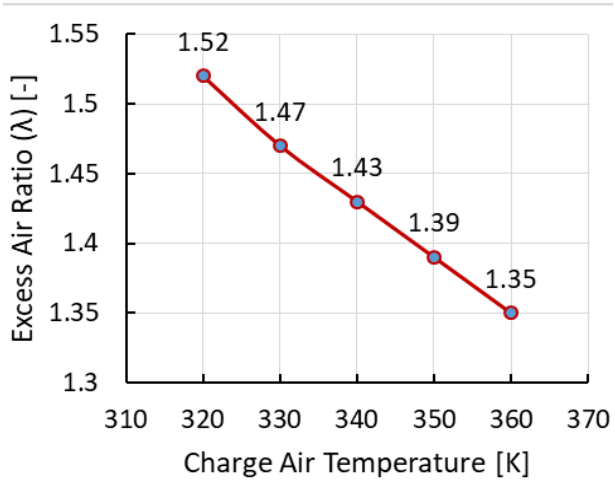

Figure 12. Excess air ratios according to CAT.

3.5. CO and CO_2 Emissions

The CO and CO_2 emissions generated inside the engine cylinder in all combustion cases are shown in figures 13 and 14, respectively. The simulation results showed a reduction tendency in both CO and CO_2 emissions when the CAT decreased. Specifically, CO and CO_2 emissions were reduced by 44.66 and 3.22%, respectively, when the CAT reduced from 360 K to 320 K. As has been well known, CO is a product of incomplete combustions while CO_2 is a product of complete combustions of hydrocarbon fuels. First, hydrocarbon fuels are oxidized to CO due to the oxidation process with O_2, and then, CO is oxidized to form CO_2 sequentially if the temperature inside the cylinder is high enough and there is still enough O_2 for oxidation. Therefore, the CO_2 formation strongly depends on the temperature and the O_2 concentration inside the engine cylinder. Meanwhile, CO formation strongly depends on the combustion quality. As shown in figure 12, the excess air ratios in all CAT cases are more than unity, meaning that there is always enough O_2 for reactive species oxidation during the combustion process. However, as the CAT decreased, the mean cylinder temperature decreased (figure 9). This is not favorable for the oxidation of CO to CO_2, causing the amount of CO_2 produced to be reduced as shown in figure 14.

Regarding the reduction of CO emission when the CAT decreased, as can be clearly seen in figure 15a, the indicated efficiency of the combustion increased as the CAT decreased. Meaning that the combustion quality was increased when the CAT decreased leading to a reduction in CO formation as shown in figure 13. In conclusion, as CAT decreased, CO formation was decreased due to higher combustion quality combined with lower In-Cylinder mean temperature inhibiting CO oxidation resulted in a reduction in CO_2 emission. This tendency was confirmed by studies in [40][41].

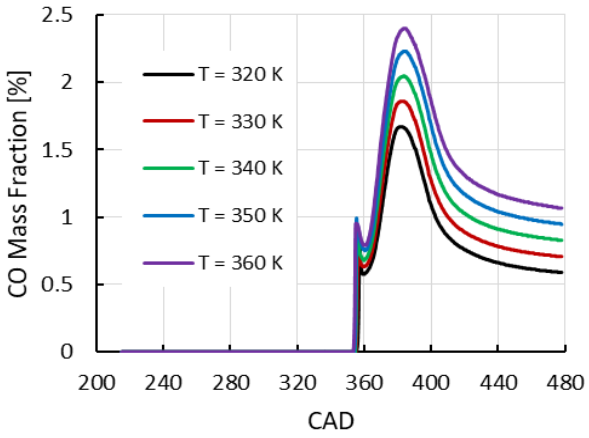

Figure 13. Mean CO mass fractions according to CAT.

3.6. Effects of the CAT on engine output

Effects of the CAT on indicated efficiency, BMEP, and BSFOC are shown in figures 15a, b, and c, respectively. As can be seen in figure 15a, the indicated efficiency was increased as the CAT decreased, resulting in an increase in the BMEP (figure 15b) and a decrease in the BSFOC (figure 15c). Specifically, the indicated efficiency was increased by 8.57% resulting in an increase in BMEP by 10.74% and a decrease in BSFOC by 9.68%, respectively, when the CAT decreased from 360 K to 320 K. The increase in the indicated efficiency could be explained as the better fuel atomization when the fuel was injected into a denser air environment in cases of lower temperatures of the charge air. The increase in BMEP and decrease in BSFOC are results of the increase in indicated efficiency.

These findings indicate many advantages of the CAT cooling method. It is not only reductions in soot, NO, CO, CO_2 emissions, and BSFOC but

also increases in indicated efficiency and BMEP. Even more amazing is these benefits can be achieved without fuel treatment or modifications in the engine, and the method can be easily applied to existing engines.

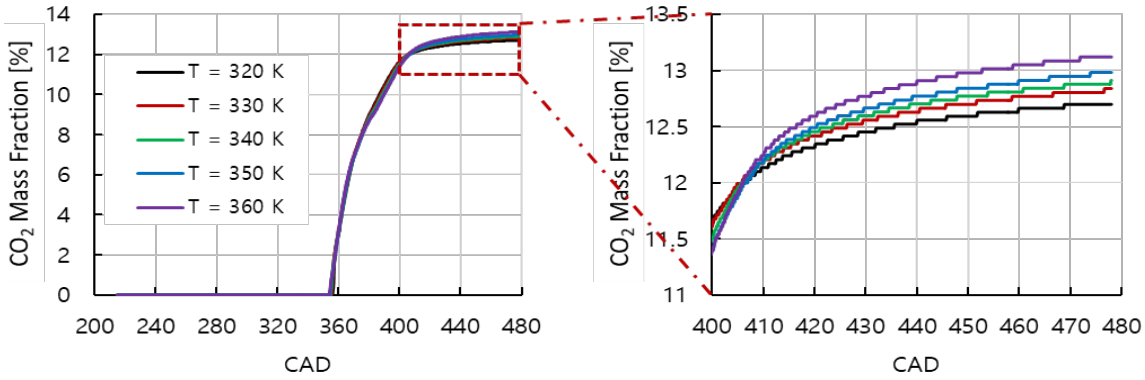

Figure 14. Mean CO_2 mass fractions according to CAT.

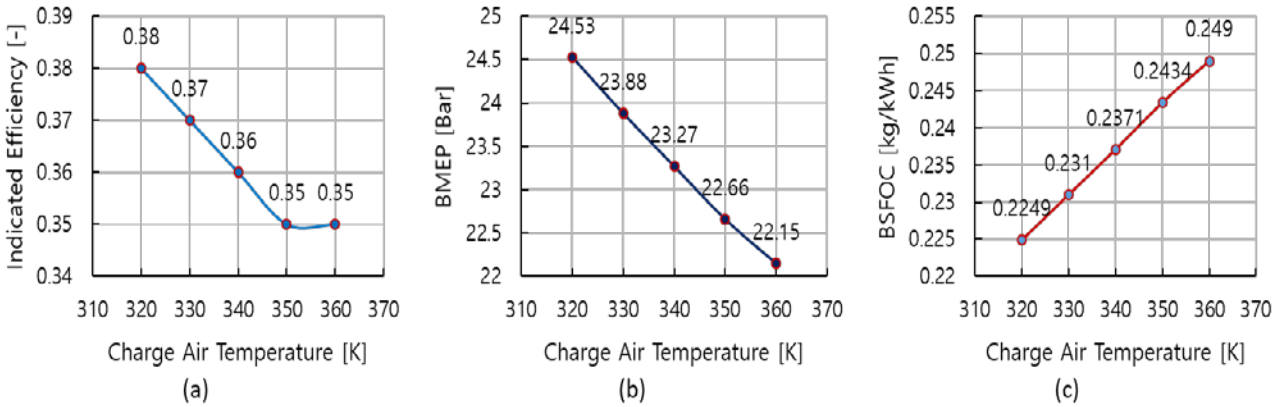

Figure 15. Indicated efficiency (a), BMEP (b), and BSFOC (c) of the engine according to CAT.

4. Conclusions

In this study, we numerically investigated the combustion process and emission characteristics inside the cylinder of a four-stroke marine generator diesel engine at full load operating with various CATs.

The major results are summarized below. When the CAT reduced from 360 K to 320 K:

- The maximum TKE decreased, implying that the turbulence velocity of the fluid flow in the engine cylinder would be decreased as the CAT decreased;
- The In-Cylinder pressure peak was increased resulting in an increase of BMEP by 10.74%;
- The In-Cylinder peak temperature was decreased, resulting in a reduction in NO emission by 33.85%;
- Soot, CO, and CO_2 emissions were also reduced by 63.92, 44.66, and 3.22%, respectively;
- The BSFOC was reduced by 9.68% due to an increase in the indicated efficiency.

This study successfully analyzed the benefits of the CAT cooling method and would be a useful material for operating existing engines in cases of trying to reduce exhaust gas emissions without any fuel treatment, modifications in the engine, or use any additional emission post-treatment device.

It only dealt with one of the two important state parameters of the charge air, the temperature, without analyzing the influence of the charge air pressure on the combustion and exhaust gas emission characteristics of the engine. So this will be the direction of future work based on this research.

Referenes

[1] H. Thomson, J. J. Corbett, J. J. Winebrake; "Natural gas as a marine fuel". Energy Policy. 2015; 87:153–167. DOI: 10.1016/j.enpol.2015.08.027.

[2] https://www.imo.org. Accessed: 19/11/2021.

[3] D.Woodward; "Pounder's Marine Diesel Engines and Gas Turbines". 9th Edition. Oxford, UK: Butterworth-Heinemann. 2009.

[4] C. J. Yang, L. Leveen, K. King; "Ethane as a cleaner Transportation Fuel". Environmental Science & Technology. 2015; 49:3263 – 3264. DOI: 10.1021/acs.est.5b00575.

[5] E. W. Kaiser, W. O. Siegl, Y. I. Henig, R. W. Anderson, F. H. Trinker; "Effect of fuel structure on emissions from a spark-ignited engine". Environmental Science & Technology. 1991; 25:2006−2012. DOI: 10.1021/es00024a004.

[6] I. V. Kanna, M. Arulprakasajothi, S. Eliyas; "A detailed study of IC engines and a novel discussion with comprehensive view of alternative fuels used in petrol and diesel engines". International Journal of Ambient Energy. 2019; 42(3):1794-1802. DOI:10.1080/01430750.2019.1614994.

[7] The Word LPG Association (WLPGA); "LPG for Marine Engines The Marine Alternative Fuel". Commercial, Passenger, Offshore Boats/Ships, Recreational Crafts and Other Boats; WLPGA Marine Group, Ireland. 2017; page 16.

[8] Y. Huang, C. J. Sung; "Effects of n-butane addition on reformer gas combustion: implications for potential of using reformer gas for an engine cold start". Proceedings of the Combustion Institute. 2002, 29(1):759 - 765. DOI: 10.1016/S1540-7489(02)80097-9.

[9] J. Huang, Y. Wang, S. Li, A. P. Roskilly, H. Yu, H. Li; "Experimental investigation on the performance and emissions of a diesel engine fueled with ethanol-diesel blends". Thermal Engineering. 2009; 29 (11-12):2484 - 2490.

[10] L. Seokhwan, O. Seungmook, C. Young, K. Kernyong; "Performance and emission characteristics of a CI engine operated with n-butane blended DME fuel". Applied Thermal Engineering. 2011; 31 (11):1929 - 1935. DOI: 10.1016/j.applthermaleng.2011.02.039.

[11] Y. Yamasaki, N. Iida; "Numerical analysis of auto-ignition and combustion of n-butane and air mixture in HCCI engine using elementary reactions". JSME International Journal. 2003, 46 (1):52 - 59. DOI: 10.1299/jsmeb.46.52.

[12] A. Saez, A. Flores-Maradiaga, M. Toledo; "Liquid butane as an alternative fuel for diesel oil burners". Applied Thermal Engineering. 2012; 45-46: 1-8. DOI: 10.1016/j.applthermaleng.2012.04.024.

[13] V. S. Babkin; "Filtrational combustion of gases-Present state of affairs and prospects". Pure and Applied Chemistry. 1993; 65(2): 335 - 344. DOI: 10.1351/pac199365020335.

[14] T. H. Fleisch, R. A. Sills, M. D. Briscoe; "Emergence of the gas-to-liquid industry: a review of global GTL developments". Journal of Natural Gas Chemistry. 2002; 11 (1):1 - 14.

[15] A. Florentius, C. Hamelinck, A. Van den Bos, R. Winkel, M. Cuijpers; "Potential of biofuels for shipping. Final Report". European Maritime Safety Agency (EMSA). Lisbon, Portugal. 2012.

[16] Y. D. Ho, Y. S. Hun, C. J. Huyk; "Experimental Study on Soot Formation in Opposed-Flow Ethylene Diffusion Flames by Mixing DME as an Alternative Fuel". Journal of the Korean Society of Marine Environment & Safety. 2010; 16(3):301-306.

[17] T. A. Semelsberger, R. L. Borup, H. L. Greene; "Dimethyl ether (DME) as an alternative fuel". Journal of Power Sources. 2006; 156 (2):497 – 511. DOI:10.1016/j.jpowsour.2005.05.082.

[18] P. V. Chien, R. B. Seok, K. J. So, L. W. Joo, C. J. Huyk. "Effects of Various Fuels on Combustion and Emission Characteristics of a Four-Stroke Dual-Fuel Marine Engine". Journal of Marine Science and Engineering. 2021; 9(10):1072. DOI: 10.3390/jmse9101072.

[19] S. J. Hwan; P. V. Chien; L. W. Ju. "Effects of the Multiple Injection Strategy on Combustion and Emission Characteristics of a Two-Stroke Marine Engine". Energies. 2021; 14 (20):6821. DOI: 10.3390/en14206821.

[20] T. Sajovaara, M. Larmi, V. Vuorinen; "Effect of CAT on E85 dual-fuel diesel combustion". Fuel. 2015; 153 (6):6-12. DOI: 10.1016/j.fuel.2015.02.096]

[21] Y. S. Huyn; L. C. Sik "Effect of undiluted bioethanol on combustion and emissions reduction in a SI engine at various charge air

conditions". Fuel. 2012; 97:887-890. DOI: 10.1016/j.fuel.2012.02.001.

[22] S. Gowthaman, A. P. Sathiyagnanam; "Effects of charge temperature and fuel injection pressure on HCCI engine". Alexandria Engineering Journal. 2016; 55 (1):119-125. 10.1016/j.aej. 2015.12.025.

[23] P. Wang; Y. Chunde; H. Guopeng, W. Hongyuan, W. Quangang; "The impact of intake air temperature on performance and exhaust emissions of a diesel methanol dual fuel engine". Fuel. 2015; 162:101-110. DOI:10.1016/j.fuel. 2015.08.073

[24] L. Eder, M. Ban, G. Pirker, M. Vujanovic, P. Priesching, A. Wimmer; "Development and Validation of 3D-CFD Injection and Combustion Models for Dual Fuel Combustion in Diesel Ignited Large Gas Engines". Energies. 2018; 11(3):643, DOI:10.3390/en11030643.

[25] P. A. Durbin; "Near-wall turbulence closure modeling without damping functions". Theoretical Computational Fluid Dynamic. 1991, 3 (1):1–13.

[26] S. Candel, D. Veynante, F. Lacas, E. Maistret, N. Darabiha, T. Poinsot; "Coherent flamelet model: Applications and current extensions". Recent Adv. Combust. Model. Recent Advances in Combustion Modelling 1990; page 19–64. DOI: 10.1142/9789814293778_0002.

[27] AVL FIRE; "Combustion Module User Manual"; AVL List GmbH, Graz, Austria. R2018a; 2018.

[28] P. V. Chien et al.; "A Numerical Study on the Combustion Process and Emission Characteristics of a Natural Gas-Diesel Dual-Fuel Marine Engine at Full Load". Energies. 2021; 14(5):1342. DOI: 10.3390/en14051342.

[29] AVL FIRE; "Spray Module User Manual"; AVL List GmbH, Graz, Austria. R2018a; 2018.

[30] AVL FIRE; "Emission Module User Manual"; AVL List GmbH, Graz, Austria. R2018a; 2018.

[31] R. Raine, C. Stone, J. Gould; "Modeling of nitric oxide formation in spark ignition engines with a multi-zone burned gas". Combustion and Flame. 1995; 102(3):241–255. DOI:10.1016/0010-2180 (94)00268-w.

[32] M. Savli; "Turbulence Kinetic Energy–TKE. Faculty of Mathematics and Physics"; University of Ljubljana. Ljubljana, SI-1000, Slovenia. 2012; vol. 9.

[33] Y. S. Huyn; L. C. Sik; "Effect of undiluted bioethanol on combustion and emissions reduction in a SI engine at various charge air conditions". Fuel. 2012; 97:887-890. DOI: 10.1016/j.fuel.2012.02.001.

[34] S. Gowthaman, A. P. Sathiyagnanam; "Effects of charge temperature and fuel injection pressure on HCCI engine". Alexandria engineering journal. 2016; 55(1):119-125.

[35] J. B. Heywood; "Internal Combustion Engine Fundamentals"; New York, USA: McGraw-Hill Education.1998.

[36] M. M. Maricq, R. E. Chase, N. Xu, P. M. Laing, The effects of the catalytic converter and fuel sulfur level on motor vehicle particulate matter emissions: light duty diesel vehicles. Environmental Science & Technology. 2002, 36 (2):283–289. DOI:10.1021/es010962l.

[37] R. T. Burnett, S. Cakmak, J. R. Brook, D. Krewski; "The role of particulate size and chemistry in the association between summertime ambient air pollution and hospitalization for cardiorespiratory diseases". Environ Health Perspect.1997; 105 (6):614–620.

[38] D. B. Kittelson, W. F. Watts, J. P. Johnson; "On-road and laboratory evaluation of combustion aerosols—Part1: Summary of diesel engine results". Journal of Aerosol Science. 2006, 37 (8): 913–930. DOI:10.1016/j.jaerosci.2005.08. 005.

[39] P. Rouncea, A. Tsolakisa, A. P. E. York; "Speciation of particulate matter and hydrocarbon emissions from biodiesel combustion and its reduction by post-treatment". Fuel. 2012, 96:90–99.

[40] A. A. Hairuddinac, T. Yusafb, A. P. Wandela; "A review of hydrogen and natural gas addition in diesel HCCI engines". Renewable and Sustainable Energy Reviews. 2014; 32:739-761. DOI: 10.1016/j.rser.2014.01.018.

[41] A. C. Alkidas; "Combustion advancements in gasoline engines". Energy Conversion and Management. 2007; 48 (1):2751-2761. DOI: 10.1016/j.enconman.2007.07.027

Ngày nhận bài: 17/01/2022
Ngày chuyển phản biện: 20/01/2022
Ngày hoàn thành sửa bài: 10/02/2022
Ngày chấp nhận đăng: 17/02/2022